JOURNAL OF MATERIALS SCIENCE **34** (1999) 3813–3819

Fabrication of gradient distribution alumina short fibre reinforced aluminium alloy

AIBIN MA
Department of Materials Science and Engineering, Southeast University, Nanjing 210096, Jiangsu, People's Republic of China

TORU IMURA, KAZUHIRO KUZUYA
Department of Mechanical Engineering, Aichi Institute of Technology, Toyota 470-03, Japan

YOSHINORI NISHIDA
National Industrial Research Institute of Nagoya, Nagoya 462, Japan
E-mail: ynishida@nirin.go.jp

Gradient distribution alumina short fibre reinforced 6061 aluminium alloy have been fabricated by taking advantage of preform compressive deformation during squeeze casting. Pressure was applied mechanically by a punch. Velocity of the punch, pre-heat temperature of the preforms and pouring temperature were controlled during the infiltration of molten 6061 alloy into alumina short fibre preforms. The distribution of hardness along the infiltration direction in the composites was measured and the distribution of volume fraction along the infiltration direction was calculated by the hardness. Velocity of the inflow, pre-heat temperature of the preform, pouring temperature of the molten metal, binder content of the preform and volume fraction of fibres, all have a very great effect on the gradient distribution of alumina short fibres in the aluminium alloy composites.

1. Introduction

The ceramic fibres reinforced aluminium alloys have excellent mechanical properties, low thermal expansion, and good wear resistance, especially at high temperature [1–4]. There are many fabrication processes for metal matrix composites (MMC) [5–7]. Most of MMC products which have been commercialized are produced by the liquid infiltration process which is called squeeze casting [8–10]. In liquid infiltration process, high pressure is applied directly to molten metal to infiltrate it into a fibrous preform. The characteristic of this process is such that this process enables one to produce not only high quality and complex shaped components efficiently, but also partially reinforced products [8, 11]. However, sometimes compressive deformation of the preform occurs during the infiltration [12, 13]. The study of the infiltration mechanism has already been theoretically and experimentally performed by Fukunaga *et al.* [14–16], Mortensen *et al.* [17–19], Clyne *et al*. [20], Nishida *et al.* [21], and other researchers. It shows that the infiltration and compressive deformation of preform are related to (a) fibre diameter and volume fraction, (b) pre-heat temperature of preform, (c) pouring temperature of molten metal, (d) velocity of inflow, (e) alignment of fibres in the preform and (f) compressive strength of fibrous preform.

In this paper, a process is presented for the fabrication of gradient distribution alumina short fibre reinforced aluminium alloy by taking advantage of preform compressive deformation during squeeze casting, which was controlled by pre-heat temperature of preform, pouring temperature of molten metal and velocity of inflow. The measurement of alumina fibre distribution in the composites along the infiltrating direction was carried out by optical micrography and measuring hardness change of the composites.

2. Experimental

2.1. Fibre preform preparation

The chemical composition and mineral composition of the alumina short fibre, produced by Electrical Chemical Industries (Japan) are given in Table I. The average diameter of the fibres is 3 μm. Tensile strength of the alumina fibre is 1760 MPa.

The preforms were fabricated using a filter apparatus. Silica series binder was used for the fabrication of fibrous preforms. The preforms used in this study were 100 mm × 70 mm by 40 mm thickness. The fibre preforms used in this study are shown in Table II.

2.2. Measurement of compressive strength of fibrous preform

Since the compressive deformation of the fibrous preform have something to do with the compressive strength of fibrous preform, the relationship between applied pressure to preforms and volume fraction of alumina fibres was measured, and shown in Fig. 1.

TABLE I Chemical and mineral composition of the alumina fibers (wt%)

Chemical composition				Mineral composition	
Al_2O_3	SiO_2	Fe_2O_3	Ig-loss	α-Alumina	Mullite
85.2	14.6	0.15	0.06	0	51

TABLE II Fibre preforms used in this study

Run number	I	II	III	IV
Binder V_b (%)	0.5	1.0	2.0	1.0
Fiber V_{f0} (%)	15	15	15	9.5

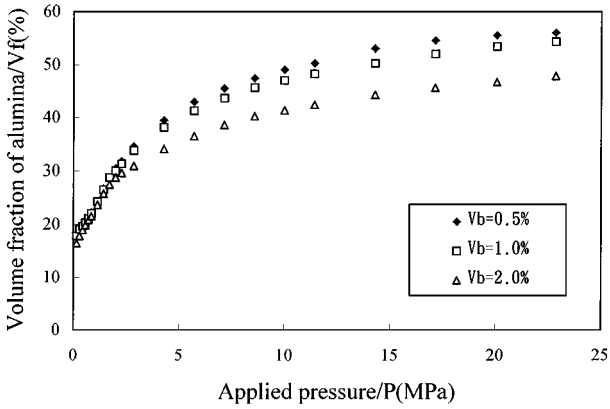

Figure 1 Relationship between applied pressure to preforms and volume fraction of alumina short fibres.

The applied pressure corresponds to the compressive strength of preforms. The volume fraction of fibres or binder content in a preform is higher, the applied pressure (strength) becomes higher. However, the effect of binder content in a preform on the change of fibre volume fraction is small, when the applied pressure is low.

2.3. Squeeze infiltration

The compressive deformation of preform is related to pre-heat temperature of preforms, pouring temperature of molten metal and velocity of inflow. So, these factors were controlled according to the conditions which are

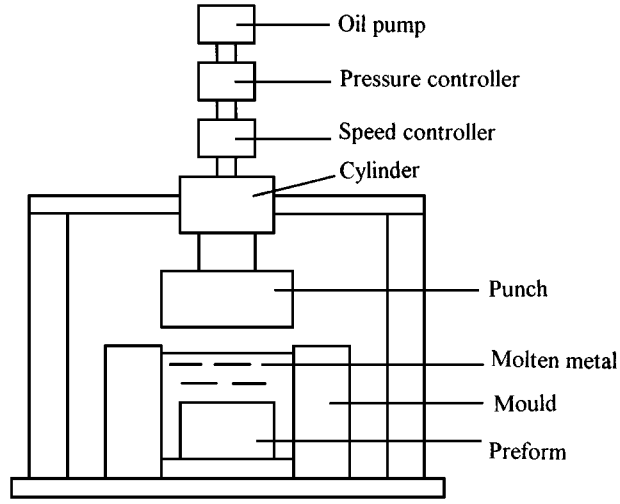

Figure 2 Experimental apparatus for squeeze infiltration.

shown in Table III. 6061 aluminium alloy was used in this study for matrix metal. The chemical composition of 6061 alloy is shown in Table IV. The infiltration apparatus used for this experiment is shown in Fig. 2. A 80 tons hydraulic press and metal mould were used. Aluminium alloy was heated to around 1033 K, and the metal mould was pre-heated to around 533 K. The pre-heated preform was set in the mould, then molten aluminium alloy was poured onto the preform, and the pressure of 100 MPa was applied by moving the punch at the set up velocity.

3. Experimental results

3.1. Structure

Fig. 3, the optical micrographs, shows the alumina fibre distribution along the infiltration direction in the composite which had 9.5% original fibre volume fraction and was infiltrated at 40 mm/s velocity of the punch. It shows that, the volume fraction of fibres at the place of 5 or 15 mm from the surface of composite is higher than that of the surface. The volume fraction is higher at 15 mm place than at 5 mm place. The pre-heat temperature of preform and the pouring temperature have some influence on the compressive deformation of the

TABLE III Technical conditions of squeeze infiltration

	I			II			III			IV		
Run number	1	2	3	1	2	3	1	2	3	1	2	3
Pre-heat temperature of preform T_f(°C)	750	750	750	300	400	550	750	750	750	750	750	750
Pouring temperature of 6061 alloy T_m(°C)	750	750	750	660	660	660	750	750	750	750	750	750
Velocity of the punch u (mm/s)	10	20	40	20	20	20	10	20	40	10	20	40
Applied pressure P (MPa)	100	100	100	100	100	100	100	100	100	100	100	100

TABLE IV Chemical composition of 6061 alloy (wt%)

Si	Fe	Cu	Mn	Mg	Cr	Zn	Ti	Al
0.40–0.80	0.70 max.	0.15–0.40	0.15 max.	0.80–1.20	0.25 max.	0.25 max.	0.15 max.	bal.

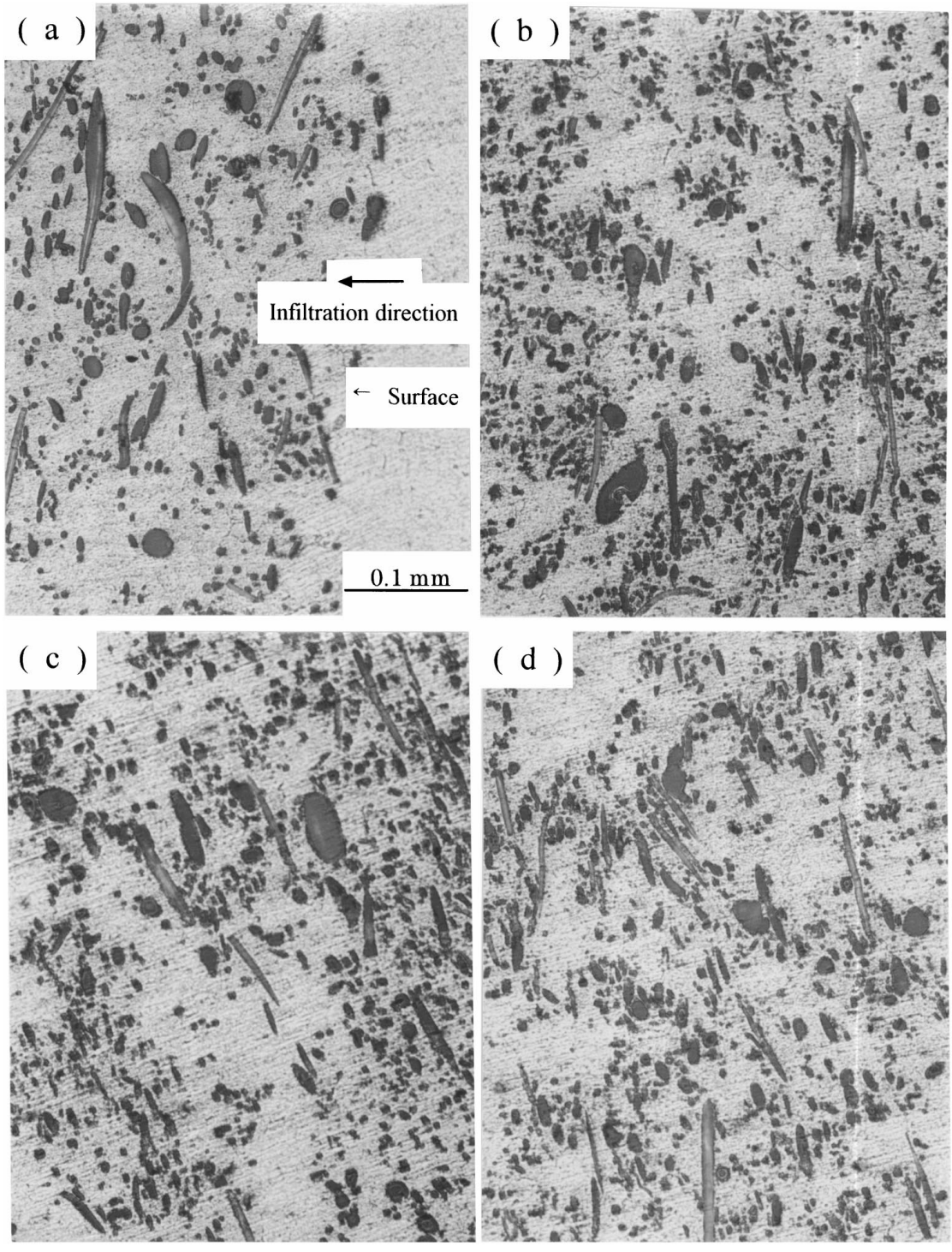

Figure 3 Optical micrographs of composites along the infiltration direction ($V_{f0} = 9.5\%$), (a) surface, (b) 5 mm from surface, (c) 15 mm from surface, (d) bottom.

preform. Fig. 4 shows the optical micrographs of the composite, which was fabricated under the conditions of pre-heat temperature 573 K and pouring temperature 933 K, along infiltration direction. It is clear that, the volume fraction of fibres increases along with the infiltration distance up to the bottom of the composite.

3.2. Hardness and volume fraction of composites along the infiltration direction

Vickers hardness distribution of the composites along the infiltration distance is illustrated in Figs 5 and 6. Fig. 5 shows that the hardness of the cases of $u = 10$ and 20 mm/s increases up to the place of 10 mm from the surface of composites, then it does not change, when the preform pre-heat temperature and the pouring temperature are 1023 K. However, the hardness of $u = 40$ mm/s increases up to 20 mm. Fig. 6 shows the effect of preform pre-heat temperature on the hardness of composites along infiltration direction. The hardness of the composites increases gradually with increasing infiltration distance and steeply near the bottom of the composites, when the preform pre-heat temperature is 573 K. However, when the preform pre-heat temperature is 673 or 823 K, the tendency of the hardness along infiltration distance is similar to the case of 573 K and

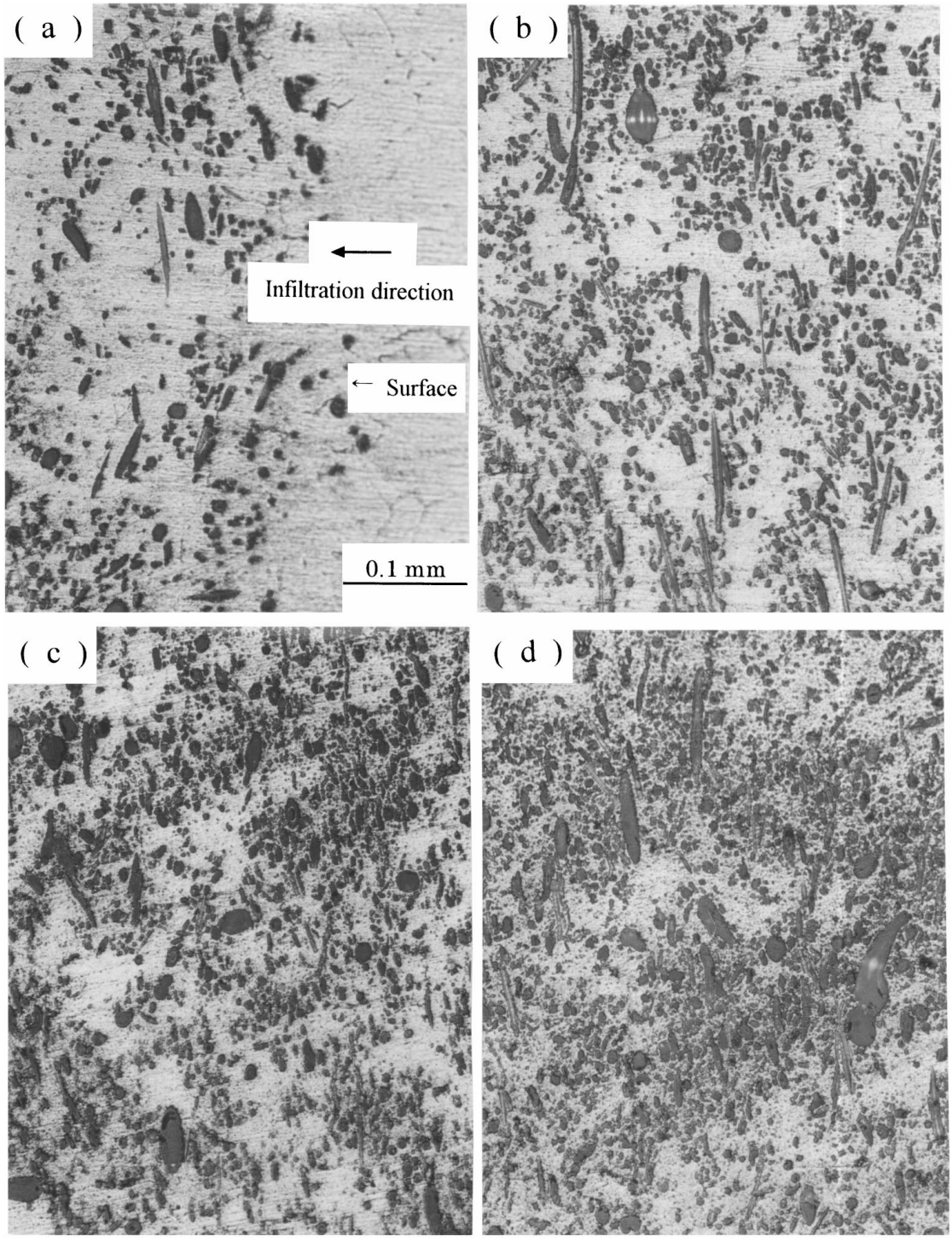

Figure 4 Optical micrographs of the composite fabricated under the condition of pre-heat temperature 573 K and pouring temperature 933 K ($V_{f0} = 15\%$). (a) surface, (b) 5 mm from surface, (c) 15 mm from surface, (d) 25 mm from surface (near bottom).

the hardness of the case of 673 K increases slightly near the bottom. In order to understand the change of fibre volume fraction in the composites clearly, data of hardness has been transformed into volume fraction of fibres in the composites. Fig. 7 shows the relationship between hardness of the composites and volume fraction of alumina fibres in the composites. By this relationship, the distribution of fibre volume fraction (V_f) was calculated from the values of hardness, and the results are shown in Figs 8 and 9. It is clear that the volume fraction of alumina fibres in these composites increases gradually along with the infiltration distance from the surface of composite up to the center of the composites, but it decreases from the center to the bottom, when the volume fraction of fibres was 9.5% and the velocity of the punch was 20 or 10 mm/s. In the case of 40 mm/s both in Figs 8 and 9, volume fraction increases more steeply from the preform surface to 20 mm depth.

3.3. Influence of binder on volume fraction

In this work, the binder contents of the preforms were 0.5, 1.0 and 2.0%. Because of that, the compressive strength of fibrous preforms is different, as shown in

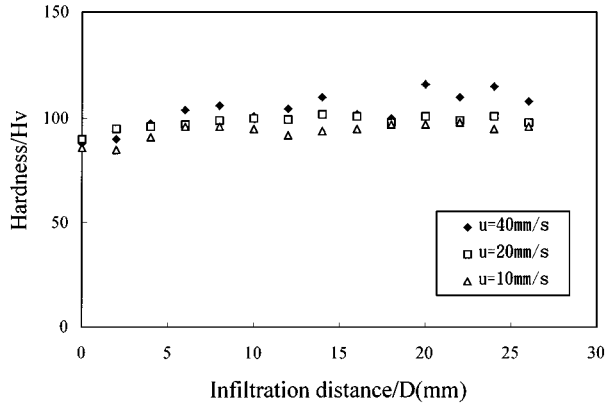

Figure 5 Relationship between hardness of the composites and infiltration distance from the surface (V_{f0} = 15%, V_b = 0.5%, T_f = 1023 K, T_m = 1023 K).

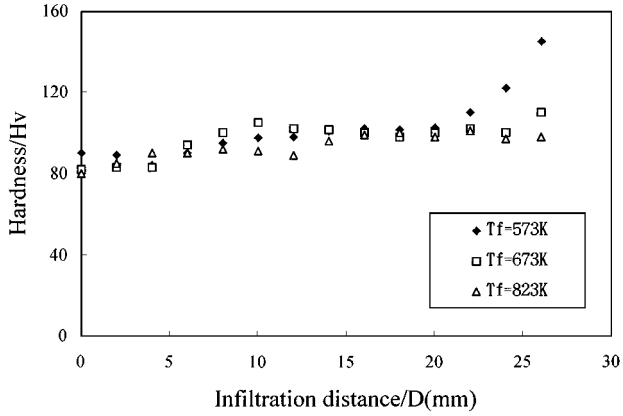

Figure 6 Relationship between hardness of the composites and infiltration distance from the surface (V_{f0} = 15%, V_b = 1.0%, T_m = 933 K, u = 20 mm/s).

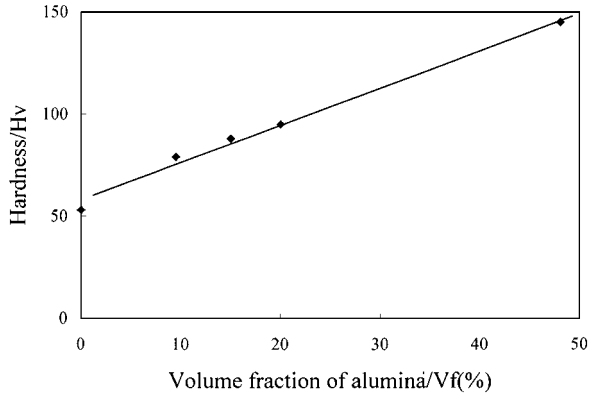

Figure 7 Relationship between hardness of the composites and volume fraction of alumina short fibres.

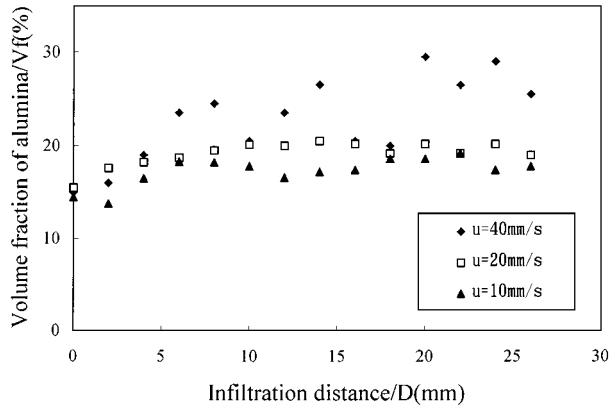

Figure 8 Relationship between volume fraction of alumina fibres and infiltration distance (V_f = 15%, V_b = 0.5%, T_f = 1023 K, T_m = 1023 K).

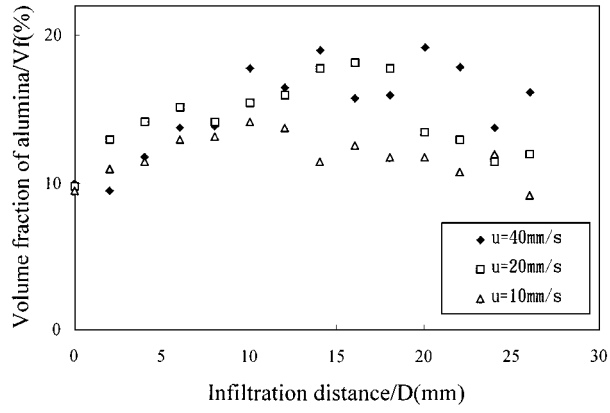

Figure 9 Relationship between volume fraction of alumina fibres and infiltration distance (V_f = 9.5%, V_b = 1.0%, T_f = 1023 K, T_m = 1023 K).

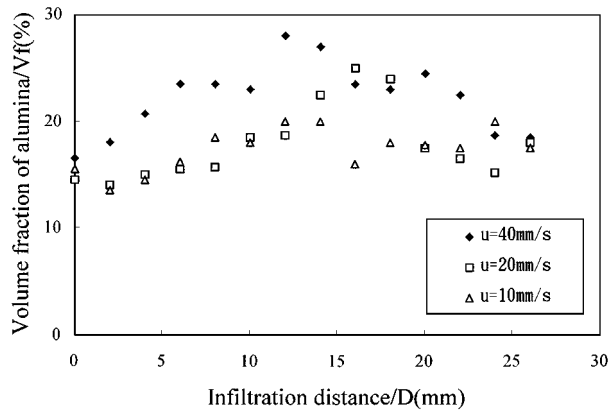

Figure 10 Relationship between volume fraction of alumina fibres and infiltration distance (V_{f0} = 15%, V_b = 2.0%, T_f = 1023 K, T_m = 1023 K).

Fig. 1. The compressive strength is high, when the binder content of the preform is high. Fig. 10 shows the relationship between volume fraction of alumina fibres and infiltration distance. In this case, binder content of the preforms was 2%, while it is 0.5% in the case of Fig. 8. The two figures show that the volume fraction of alumina fibres of $u = 40$ mm/s increases initially in both Figs 8 and 10, and it stops and decreases at the center of composites. The increase of volume fraction of $u = 20$ and 10 mm/s is little in both cases of the binder content.

4. Discussion

4.1. Calculation of the pressure applied to preform

When composites are produced by squeeze casting, the velocity of the punch is controlled. Then, the inflow velocity of molten metal into a preform is determined by the punch velocity. The pressure P_s which is applied to a preform starts to rise from zero when the punch comes down and contacts with molten metal, and is given before the start of preform deformation by [21]

$$P_s = \frac{\mu u(1-F)}{K_0'(1-V_{f0}')}\int_0^t u\,dt - \frac{4V_{f0}\gamma\cos\theta}{d_f(1-V_{f0})} \quad (1)$$

where t is time, μ is viscosity, u is volume of fluid flowing per unit time and unit cross-sectional area of porous media and defined by Darcy's law, F is the volume fraction of the solid metal, V_{f0} is the original volume fraction of fibres, V_{f0}' is $V_{f0}+(1-V_{f0})F$, γ is the surface energy, θ is the contact angle between fibre and molten metal, d_f is the diameter of the fibre and K_0' is the permeability, which can be calculated by

$$\frac{K_1}{R^2} = \frac{1}{4V_{f0}'}\left(-\ln V_{f0}' - \frac{3}{2} + 2V_{f0}' - \frac{V_{f0}'^2}{2}\right) \quad (2)$$

$$\frac{K_2}{R^2} = \frac{1}{8V_{f0}'}\left(-\ln V_{f0}' + \frac{V_{f0}'^2-1}{V_{f0}'^2+1}\right) \quad (3)$$

$$K_0' = \tfrac{1}{2}(K_1+K_2) \quad (4)$$

where R is the radius of fibre.

The second term of Equation 1 corresponds to the threshold pressure which is needed to start the infiltration of molten metal.

If there is no solid when the molten metal infiltrates the preform, F will be zero. Supposing $\gamma = 0.893$ Pa·m, $\theta = 160$ deg, $d_f = 3\times10^{-6}$ m, $\mu = 1.0\times10^{-2}$ Pa·s, and set up velocity of the punch is constant, the relationship between the pressure P_s and time t is shown in Figs 11 and 12 from Equation 1. P_s is the actual pressure which compresses the preform. If the pressure P_s is higher than the threshold pressure at a certain time, the infiltration of molten metal into the fibrous preform starts and continues. If the applied pressure is higher than the compressive strength of the preform (shown in Fig. 1) at a certain time, the compressive deformation will start.

Fig. 11 shows that when the velocity (u) of the punch is low, the pressure P_s is much lower than that of the high punch velocity. If the velocity of the punch is high, the pressure P_s increases steeply and compresses the preform rapidly. The compressive deformation of a preform is much easier at the high velocity of a punch as shown in Figs 8 and 9. Fig. 12 shows the effect of the volume fraction of alumina fibres on the pressure P_s. The volume fraction is higher, P_s is higher, too.

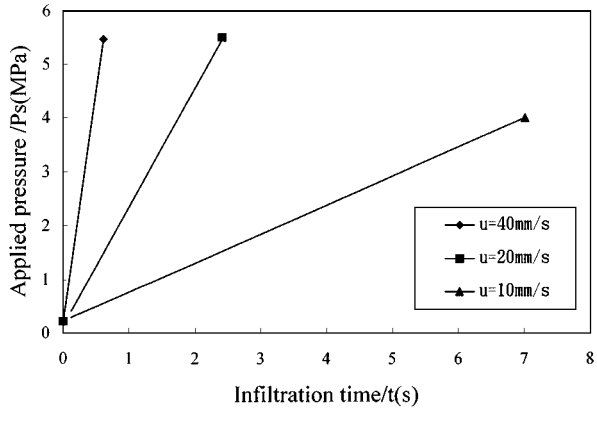

Figure 11 Relationship between applied pressure and infiltration time ($V_f = 15\%$).

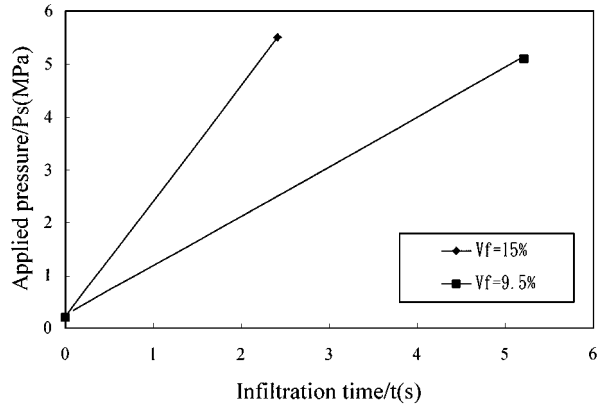

Figure 12 Relationship between applied pressure and infiltration time ($u = 20$ mm/s).

4.2. Effect of pouring temperature and pre-heat temperature of preform

In Equation 1, if there is no solid, F will be zero, and V_{f0}' will be V_{f0}. However, if the pouring temperature of molten metal and pre-heat temperature of preform are lower than the melting point, a part of molten metal will freeze in the preform during infiltration. In this work, one kind of pouring temperatures of molten metal is 933 K, and pre-heat temperatures of the preforms are 573, 673 and 823 K. The solidification temperature of 6061 aluminium alloy is 925–955 K. In this condition, a part of molten aluminium alloy will freeze when the molten metal is infiltrating the preform of alumina fibres. Heat exchange between molten metal and fibres is expressed by following equation.

$$V_f\rho_f C_f(T_M - T_f) = (1-V_f)\rho_m F H + (1-V_f)\rho_m C_m(T_m - T_M) \quad (5)$$

where T_f, T_m are the initial temperatures of the preform and molten metal, T_M is the solidification temperature of the molten metal, ρ_f and ρ_m are the densities of fibre and molten metal, C_f and C_m are the specific heat of fibre and molten metal, H is the latent heat of molten metal. When the pouring temperature is 933 K, the T_m is almost equal to T_M (925 K), the volume fraction of the solid can be given by Equation 6

$$F = \frac{V_f\rho_f C_f(T_M - T_f)}{(1-V_f)\rho_m H} \quad (6)$$

Supposing $\rho_f = 3.4$ g/cm^3, $C_f = 0.19$ cal/kg·K, $\rho_m = 2.7$ g/cm^3, $H = 393.56$ J/kg, $V_{f0} = 15\%$ and $T_M = 925$ K in Equation 6, F can be calculated, when the pre-heat temperatures of fibrous preforms are 573, 673 and 823 K. Because the latent heat (H) of molten metal is much larger than the specific heat (C_f) of fibres, solid metal is little in the infiltration of molten metal into the fibrous preform. When the initial fibre preform temperature, T_f, and the pouring temperature of molten metal are sufficiently low, solid metal forms at the infiltration

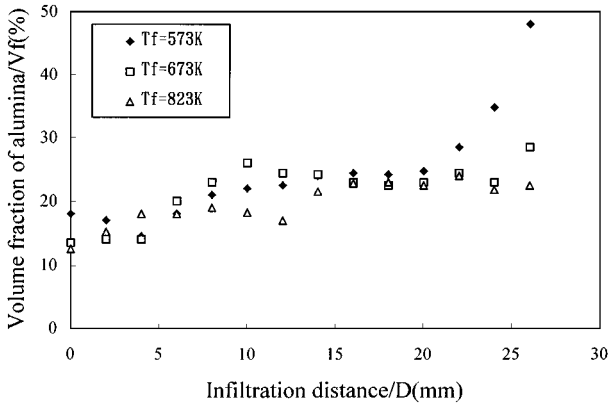

Figure 13 Effect of the pre-heat temperature of preform on the alumina volume fraction in the composites ($V_{f0} = 15\%$, $V_b = 1.0\%$, $T_m = 933$ K, $u = 20$ mm/s).

front and remains at the point where it has formed in the form of a coating surrounding the fibres. The effect of pre-heat temperature of preform on the compressive deformation of the preform is shown in Fig. 13. The volume fraction of fibres in this composite increases gradually along with the infiltrating distance from the surface to the bottom of the composite when the pre-heat temperature of the preform is 573 K. Because the velocity of punch is 20 mm/s, only half of 40 mm/s, the volume fraction of fibres in the middle of the infiltration distance is lower than that of the velocity 40 mm/s of the punch (shown in Fig. 8), but it is much higher at the end of the infiltration distance of the composite than that of the 40 mm/s. When the pre-heat temperature of preform is higher than 673 K, the effect on the volume fraction of fibres is similar to that of 923 K fibre pre-heat temperature.

5. Conclusion

Gradient distribution alumina short fibre reinforced 6061 aluminium alloy has been fabricated by taking advantage of preform compressive deformation during the squeeze infiltration. The following points have been clarified by experiments and theoretical analysis.

1. By controlling the velocity of inflow, pre-heat temperature of the preform and pouring temperature of molten metal, gradient distribution alumina short fibre reinforced aluminium alloy can be fabricated.

2. The effect of velocity of inflow (u) on the distribution of volume fraction of fibres is great. When the u is high, the volume fraction of fibres in the composite is high.

3. The binder content of a preform influences the compressive deformation of the preform. If the binder content is lower, the compressive deformation is larger.

4. The effect of pre-heat temperature (T_f) of the preform on the distribution of fibres is great, when T_f is lower than 673 K and pouring temperature of molten metal is close to the solidification temperature of the metal.

5. The fabrication of the gradient distribution short fibre reinforced 6061 aluminium alloy is difficult when the volume fraction of fibres is low.

Acknowledgement

Authors would like to express their thanks to Mr. K. Ikemoto for his assistance in experimental works.

References

1. T. DONOMOTO, N. MIURA, K. FUNATANI and N. MIYAKE, SAE Paper, 830252, 1983.
2. T. KOMATSUBARA, M. OKAJIMA, Y. KOYASUKATA and H.HOSHINO, *Sanyo Technical Review* **20** (1988) 107.
3. JIANQING JIANG, AIBIN MA, HUANAN LIU and RONGSHENG TAN, *Wear* **171** (1994) 163.
4. K. FUKIZAWA and H. SHIINA, *J. Soc. Automotive Engi Japan* **46** (1992) 66.
5. A. SATO and R. MEHRABIAN, *Met. Trans.* **7B** (1976) 443.
6. M. YOSHIDA, *SAMPE* **24** (1979) 1417.
7. A. M. PATTON, *J. Ins. Metals* **100** (1972) 197.
8. K. F. SAHM, *Verbundewerkst Tag* **1** (1974) 269.
9. H. MATSUBARA, Y. NISHIDA, I. SHIRAYANAGI and M. YAMADA, *J. Inst. Light Metal Japan* **39** (1989) 338.
10. JIANQING JING, HUANAN LIU, AIBIN MA and RONGSHEN TAN, *J. Mater. Sci.* **29** (1994) 3767.
11. T. HAYASHI, H. USHIO and M. EBISAWA, SAE Technical Paper, 890557, 1989.
12. T. YAMAUCHI and Y. NISHIDA, *J. Japan Inst. Metals* **58** (1994) 552.
13. *Idem. ibid.* **58** (1994) 1436.
14. FUKUNAGA and M. KURIYAMA, *J. Japan Soc. Mech. Eng.* (*c*) **47** (1981) 1207.
15. FUKUNAGA and K. GODA, *ibid.* **49** (1983) 1808.
16. *Idem., J. Japan Inst. Metals.* **49** (1985) 78.
17. A. MORTENSEN, L. J. MASUR, J. A. CORNIE and M. C. FLEMINGS, *Met. Trans. A* **20A** (1989) 2535.
18. *Idem., ibid.* **20A** (1989) 2549.
19. A. MORTENSEN and T. WONG, *ibid.* **21A** (1990) 2257.
20. T. W. CLYNE, M. G. BADER, G. R. CAPPLEMAN and P. A. HURBERT, *J. Mater. Sci.* **20** (1985) 85.
21. T. YAMAUCHI and Y. NISHIDA, *Acta Metal. Mater.* **43** (1995) 1313.

Received 6 March 1997
and accepted 8 February 1999